International Journal of Multiphase Flow 35 (2009) 507–515

Contents lists available at ScienceDirect

International Journal of Multiphase Flow

journal homepage: www.elsevier.com/locate/ijmulflow

Flow of oil–water emulsions through a constricted capillary

S. Cobos [a], M.S. Carvalho [a,*], V. Alvarado [b]

[a] PUC-Rio, Department of Mechanical Engineering, Rua Marques de São Vicente 225, Gávea, 22453-900 Rio de Janeiro, RJ, Brazil
[b] University of Wyoming, Department of Chemical and Petroleum Engineering, Dept. 3295, 1000 E. University Avenue, Laramie, WY 82071, USA

ARTICLE INFO

Article history:
Received 30 October 2008
Received in revised form 4 February 2009
Accepted 23 February 2009
Available online 12 March 2009

Keywords:
Emulsions
Micro-capillary
Enhanced-oil recovery
Porous media
Pore blockage
Mobility control

ABSTRACT

The flow of oil-in-water emulsions through quartz micro-capillary tubes was analyzed experimentally. The capillaries were used as models of connecting pore-throats between adjacent pore body pairs in high-permeability media. Pressure drop between the inlet and outlet ends of the capillary was recorded as a function of time, for several values of the volumetric flow rate. Several distinct emulsions were prepared using synthetic oils in deionized water, stabilized by a surfactant (Triton X-100). Two oils of different viscosity values were used to prepare the emulsions, while two distinct drop size distributions were obtained by varying the mixing procedure. The average oil drop size varied from smaller to larger than the neck radius. The results are presented in terms of the extra-pressure drop due to the presence of the dispersed phase, i.e. the difference between the measured pressure drop and the one necessary to drive the continuous phase alone at the same flow rate. For emulsions with drops smaller than the capillary throat diameter, the extra-pressure drop does not vary with capillary number and it is a function of the viscosity ratio, dispersed phase concentration and drop size distribution. For emulsions with drops larger than the constriction, the large oil drops may partially block the capillary, leading to a high extra pressure difference at low capillary numbers. Changes in the local fluid mobility by means of pore-throat blockage may help to explain the additional oil recovery observed in laboratory experiments and the sparse data on field trials.

1. Introduction

Emulsions, namely liquid–liquid dispersions, are ubiquitous to oil production operations. Most crude oil in the World is in fact produced as water-in-oil (more commonly) or oil-in-water (generally at high water cut) emulsions. Certain crude oils contain enough naphthenic acid fractions as to generate natural surfactants upon addition of alkaline components to serve as stabilizing agent, as discussed by Kokal (2005). In practice, synthetic surfactants are frequently added to oil–water systems to lower interfacial tension and hence stabilize emulsions. Typical configurations of an emulsion are: oil-in-water, water-in-oil or a more complex dispersion, for instance a dispersed-phase siting inside each droplet already dispersed in a continuous phase, such as the case oil-in-water-in-oil emulsions.

Emulsions play an important role in many enhanced-oil recovery (EOR) processes, particularly in chemical flooding involving alkaline components or surfactants, because emulsions are frequently formed as a result of the injection of chemical blends into oil-bearing reservoirs. Emulsions are also important in surfactant-enhanced aquifer remediation of subsurface zones contaminated with organic liquids (Jain and Demond, 2002). Formation damage by viscous emulsions during oil production operations reduces well productivity. On the other hand, as discussed by Romero et al. (1996) and Bai et al. (2000), the ability of emulsions to block water channels can be exploited to control water production in heterogeneous formations. Seright and Liang (1995) summarized the advantages and disadvantages of different blocking agents, including emulsions. According to their review, emulsions would approach placement properties similar to those of a low-viscosity gelant. Recent field results presented by Bai et al. (2000) showed the potential of emulsions as well conformance agents. A number of authors agree that the observed blocking mechanisms can be attributed in part to the pressure drop–flow rate response of emulsion flow in porous media (Bai et al., 2000; Khambhratana et al., 1998). Partial pore blocking by emulsions can be associated with the so-called straining, a mechanism directly controlled by the ratio of droplet to pore-throat radii, or interception for the case of small droplets. However, models for emulsion flow in porous media often rely on apparent rheological response, to explain the dynamic behavior of emulsion flow. It is clear that the flow in the pore scale cannot be described by an effective viscosity. More realistic two-phase flow models to describe the emulsion flow in the pore scale are necessary.

It is our contention that despite the progress in the study of emulsion flow in porous media, detailed analysis at the pore-scale

* Corresponding author. Tel.: +55 21 3527 1174; fax: +55 21 3527 1165.
E-mail address: msc@puc-rio.br (M.S. Carvalho).

0301-9322/$ - see front matter © 2009 Elsevier Ltd. All rights reserved.
doi:10.1016/j.ijmultiphaseflow.2009.02.018

is still required to develop reliable models of emulsion flow through porous media. Sarma et al. (1998) visualized emulsified solvent flooding for heavy oil recovery and clearly pointed out that emulsion mobility in porous media is not directly related to emulsion viscosity. Instead, trapping of emulsions droplets at pore throats is the dominant mechanism in mobility control by oil-in-water emulsions. Results in bead-packed visual models showed the apparent mobility control exerted by the emulsified solvent, reflected also as better heavy-oil recovery. Experiments with Ottawa sand packs showed that mobility control can be an important recovery mechanism for emulsion flooding. Therefore, understanding how emulsion flows through a porous media is not only relevant to describe the effective single-phase flow behavior, but also will help shed light on the oil recovery mechanisms in emulsion flooding.

This paper presents visualization and pressure drop measurements of oil-in-water emulsions flowing through a glass model of an expansion–contraction–expansion micro-capillary tube. The physical model is intended to mimic a pore-throat connecting two adjacent pore-bodies of a high permeability porous media. Emulsions prepared with mineral or synthetic oils and a surfactant solution were pumped through the glass capillary and the pressure response was recorded as a function of time for a range of imposed flow rates. The extra-pressure drop due to the presence of the dispersed phase was determined as a function of operating conditions and liquid properties, indicating the range of parameters at which partial blocking of the pores could be observed. The results can be used in the development of a capillary network model to study the flow of emulsions through a porous medium.

Before describing the experimental analysis and results of this work, we discuss some of the past work directly related to flow of emulsions in porous media and analysis of the flow of a single drop through straight and constricted capillaries.

1.1. Experiment and models for emulsion flow through porous media

Romero et al. (1996) carried out a three-stage study to develop a deep-penetrating oil-in-water emulsion to improve sweep efficiency in heterogeneous and fractured formations. The average emulsion droplet size used was 2.10 μm, obtained by mixing the oil with an alkaline solution. The idea of flooding the pore space with droplet diameter similar to rock pore-throat size was presented earlier by McAuliffe (1973b). The injectivity index in the experiments of Romero et al. (1996) with consolidated rock dropped 96–99% of its original value and the emulsion maintained its plugging ability even after the injection of 27 PV of water. Bai et al. (2000) presented the results of an emulsifying treatment yielding viscous emulsions for water shutoff applied to 238 wells in Liaohe field, China, in the period from 1991 to 1999. An 83.6% success rates was reported, with an average effective term of 4.5 months.

McAuliffe (1973b) carried out experiments with oil-in-water emulsions, between 10% and 80% oil fraction, using three crude oils, and sodium hydroxide as the caustic agent (alkaline component). Emulsion viscosity was low for an oil fraction $\leqslant$50%, because water was the continuous phase. Apparent permeability after emulsion injection in a 1360 mD-core was a strong function of the mean droplet size. Significant drop in permeability was observed for average droplet diameter of 12 μm. In all cases, plugging stopped once the reduction in permeability reached 1–10% of the original rock permeability value. McAuliffe related this result to the threshold pressure drop across the length of a pore throat necessary to mobilize a droplet through the throat. Oil recovery with emulsion flooding in cores was attributed to corrections of heterogeneity in the rock, and not to miscibility. This was perhaps the first time that emulsion flooding was proposed for EOR purposes. McAuliffe (1973a) described a field pilot test at the 5K of the Midway–Sunset oil field in California, in which 33,000 bbl of emulsion were injected. This field trial is the first significant reported case of EOR based on macroemulsion flooding. A total of additional 55,000 bbl of oil were attributed to 0.4% PV, 14%-oil emulsion treatment. The results indicate better sweep efficiency of water chasing an emulsion bank, with lower water-oil ratio (WOR) in production wells.

Early work by Alvarado and Marsden (1979) presented an analogy between rheograms in capillary tubes and pressure drop–flow rate (superficial velocity) response of emulsion flow in rock samples to develop a rheological model of macroemulsions in porous media. Oil-in-water macroemulsions prepared with mineral oil, water and a surfactant were shown to behave as Newtonian fluids at a volumetric dispersed phase concentrations less than 50%. At higher concentration values, the emulsions became pseudo-plastic. A fitting procedure was developed to bring porous media rheograms to match capillary tube rheograms. A critical dispersed-phase concentration, between 40% and 50% in their experiments, was found to be a function of the emulsifier concentration. A modified Darcy law, accounting for permeability reduction by plugging, was used to describe the flow behavior of oil-in-water Newtonian macroemulsions in porous media.

Soo and Radke (1984) studied the flow of stable oil-in-water emulsions through porous media, by using emulsions with average droplet diameters of 2, 3, 5, 7 and 10 μm, flowing through two Ottawa sandpacks with mean pore-throat diameters of 17.3 and 29.5 μm, respectively. Micromodel experiments were also carried out, in which Ottawa sand was sandwiched between glass plates. They clearly showed that, besides the straining of large droplets in pore throats, interception in crevices or pockets between grains was also a capture mechanism. The authors developed a filtration model for dilute emulsions (Soo and Radke, 1986; Soo et al., 1986). Deep-bed filtration theory concepts were used to describe dilute, stable emulsion flow in porous media, including flow redistribution and large permeability reductions (see Soo and Radke, 1986). The important parameters in the model are λ_p (the filter coefficient) and β_p (which measures the effectiveness of the retained drops in pores of throat diameter D_p). The former parameter determines the droplet capture, while the latter one controls permeability reduction. These parameters, for lack of theoretical treatment, were determined empirically, leading to the concept of flow diversion, characterized by a parameter α. Darcy law completed the model. Soo et al. (1986) showed how to estimate filtration parameters of their model from experimental data. Emulsions ranging from 0.5% to 2.5% dispersed phase concentrations were used to test the filtration theory for emulsion flow in porous media. The model successfully described emulsion flow results up to approximately 1% concentration of the dispersed phase.

Hofman and Stein (1991) presented experimental results on the influence of electrostatic repulsion and emulsion stability on the permeability impairment caused by emulsion flow through porous media. The dispersed-phase concentration was 1% (v/v) in all their experiments. Significant permeability reduction was observed for average droplet diameter equal to 5.1 and 8.9 μm, respectively, being larger for the larger average diameter. Hofman and Sten report this as a striking result, because the pore-size distribution had a large fraction of all the pores well above the average droplet size. The results indicate that both stable and unstable emulsion caused permeability reduction, being the latter more effective in plugging porous media.

Islam and Farouq Ali (1994) developed a Darcy-level model for flow of stable emulsions in porous media, including in situ generation. Their model was based on conservation equations for water, oil and emulsion phases, coupled to a transport equation. The filtration model of Soo and Radke (1984, 1986) was used to account

for capture mechanisms. The results were compared to the experimental data of Soo and Radke (1984).

Abou-Kassem and Farouq Ali (1995) reviewed pseudo-plastic fluid models of emulsion flow in porous media and discussed their underlying assumptions. They proposed a Darcy-law type model based on the flow of a power-law liquid through a bundle of tubes. The mapping of porous-media rheograms on capillary-tube type rheograms followed from Alvarado and Marsden (1979).

Khambhratana et al. (1997) developed a simulator for flow of emulsions in porous media and compared the results with experimental data obtained in Berea and an Ottawa sand pack core floods presented by Khambhratana et al. (1998). The best match between simulation results and experimental data were obtained when a multiphase non-Newtonian rheological model of an emulsion with interfacial tension-dependent relative permeability curves and time-dependent capture were used.

As for the review presented, it appears that an accurate model for flow of emulsions in porous media is still not available. A better understanding of the flow of drops immersed in a continuous liquid phase through a constricted capillary is crucial in this development. In the following sub-section, we discuss some of the first attempts in this direction.

1.2. Flow of a single drop immersed in a continuous phase through straight and constricted capillaries

The flow of a single drop immersed in the liquid flowing through a straight capillary was analyzed experimentally by Ho and Leal (1975) and Olbricht and Leal (1982). They measured the extra pressure drop due to the presence of a single drop in the flow as a function of the ratio between the drop diameter and the capillary diameter, viscosity ratio and flow rate (capillary number). The same situation was studied using a boundary integral method by Martinez and Udell (1990). For small drops, e.g. ratio of drop diameter to tube diameter less than 0.7, the extra pressure drop does not depend on the capillary number. For drops larger than the tube diameter, the extra pressure drop falls with capillary number and rises with viscosity ratio. The extra pressure drop is negative when the drop is less viscous than the continuous phase, and positive in the reverse case. The extra pressure difference is a strong function of the drop to capillary diameter ratio d/D. Martinez and Udell (1990) have shown that for $d/D \lesssim O(1)$, the extra pressure difference scales with $(d/D)^5$. For drops much larger than the capillary diameter, i.e. $d/D \gg 1$, Ho and Leal (1975) observed that the increase in the extra pressure difference with the drop diameter can be predicted simply by the taking into account the increase in length of the large drop.

Olbricht and Leal (1983) reported experimental results on the flow of a single drop immersed in a liquid flowing through a horizontal tube with periodically varying diameter. As the drop flows through the converging–diverging channel, the pressure difference oscillates. Each oscillation of the pressure signal corresponded to a drop's passage through a constriction. The extra-pressure difference response was characterized by the arithmetic average of the signal and the amplitude of the oscillation. The results are analyzed separately for low and for high capillary regimes. At low capillary number, the analysis was restricted to drops less viscous than the continuous phase. For drops smaller than the capillary constriction, the pressure oscillation was smaller than the uncertainty of the measurements, but it rises with the drop diameter, being relevant when the drop is larger than the constriction diameter. The extra-pressure difference was higher at low capillary number, when all the other flow parameters were kept the same. At a fixed capillary number, the extra-pressure difference was positive for small drops, but falls and becomes negative as the drop size rises. Olbricht and Leal (1983) discuss that the extra-pressure difference is determined by competing mechanisms, such as the deformation of the drop, interaction between the drop and the wall and the simple replacement of suspending liquid by a dispersed phase liquid of different viscosity. At high capillary numbers, they explored situations with drops less and more viscous than the suspending liquid. For all cases explored, both small and large drops, the oscillation of the pressure signal was very small and the extra-pressure difference did not vary much with capillary number, but was a strong function of the viscosity ratio between the phases and the drop size.

The pressure oscillation due to the flow of a single drop through a constricted capillary was predicted by the analysis presented by Tsai and Miksis (1994) using a boundary integral method.

It is important to note that all the experimental results discussed in the previous paragraphs were obtained with tubes with diameter in the order of 1–5 mm, much larger than the flow channels in a porous media. Moreover, the range of capillary number explored, $10^{-2} < Ca < 1$, is also outside the typical local capillary number in a pore flow. In this work, we extend these analyses to micro-capillaries, with constriction diameter of 50 μm, and much lower capillary numbers. Since we are interested in understanding the fundamental oil-recovery mechanisms upon emulsion injection, we focus our analysis on drops more viscous than the continuous phase, range not explored in the literature at the low capillary number regime.

2. Materials and methods

2.1. Materials

Five oil-in-water emulsions were prepared for the experiments, as shown in Table 1. The continuous phase was a dilute solution of Carbopol (a low molecular weight polymer), with a concentration equal to 0.1 wt%, in deionized water. The polymer was added to increase the continuous phase viscosity and therefore delay the segregation of phases due to density differences. The aqueous solution presented a shear thinning behavior, and its viscosity at $\dot{\gamma} = 0.01\ s^{-1}$ was $\eta \approx 0.2$ Pa s. A surfactant was added to the aqueous phase to lower the oil–water interfacial tension and limit the coalescence of oil drops. A nonionic surfactant, Triton X-100, was used to avoid pH changes of the polymeric solution and therefore changes in its viscosity. The surfactant concentration was approximately 10 times the critical micelle concentration. Two synthetic oils were used as the dispersed phase. The first oil was SHELL Tivela 160, with density and viscosity equal to $\rho_o = 993\ kg/m^3$ at 20 °C and $\mu_o = 350$ cP at 25 °C, respectively. The second oil used was SHELL Tivela 460, with density and viscosity equal to $\rho_o = 997\ kg/m^3$ at 20 °C and $\mu_o = 950$ cP at 25 °C, respectively. The interfacial tension of both oils with respect to the continuous phase was $\sigma = 5$ mN/m. Each oil and water + polymer + surfactant mixture was sheared in a homogenizer (Ultramax). The rotation of the dispersing tool and the time of mixture were used to control the drop size distribution of the emulsion. A sample of each emulsion was placed under an optical microscope and the size of

Table 1
Main properties of the oil-in-water emulsions used in the experiments.

Emulsion	Internal phase	μ_o (cP)	Concentration	Drop size
1S	Tivela 160	350	30/70	Small
1L	Tivela 160	350	30/70	Large
2S	Tivela 460	950	30/70	Small
2L	Tivela 460	950	30/70	Large
3S	Tivela 460	950	60/40	Small

individual drops was measured to build the normalized histogram of drop size distribution.

One emulsion set was prepared by dispersing oil in water using a rotation rate of 26,500 rpm for 3 min. The largest drop diameter of the dispersed phase was approximately 35 μm, smaller than the capillary throat diameter. Emulsions prepared with this procedure were labelled *S. A second emulsion batch was obtained by mixing a fraction of the emulsion generated at a rotation of 6500 rpm for 3 min and the remaining fraction obtained by hand-shaking an oil–water mixture. This procedure led to a very broad dispersed phase diameter distribution, containing drops much larger than the capillary constriction. These emulsions were labelled *L. Fig. 1 shows the normalized histograms of all the five emulsions tested. As expected from optical determinations of drop-size distributions, the frequency corresponds to drop numbers. The volume fraction of large drops is under represented, being much larger than that of small drops. The mean and the standard deviation of the drop size distribution of the five emulsions are presented in Table 2.

The first two emulsions, labelled 1L and 1S, were prepared using SHELL Tivela 160, with an oil fraction of 30%. The difference between emulsions 1L and 1S was the drop size distribution. Emulsion 1L had large drops, while 1S consisted of small drops. Emulsions 2L and 2S were prepared at 30% oil concentration, but using oil SHELL Tivela 460, instead. Similarly, 2L contained large drops and 2S small drops. In order to determine the effect of the dispersed phase concentration, an emulsion with small drops, but with 60% of oil, was prepared. This emulsion was labelled 3S.

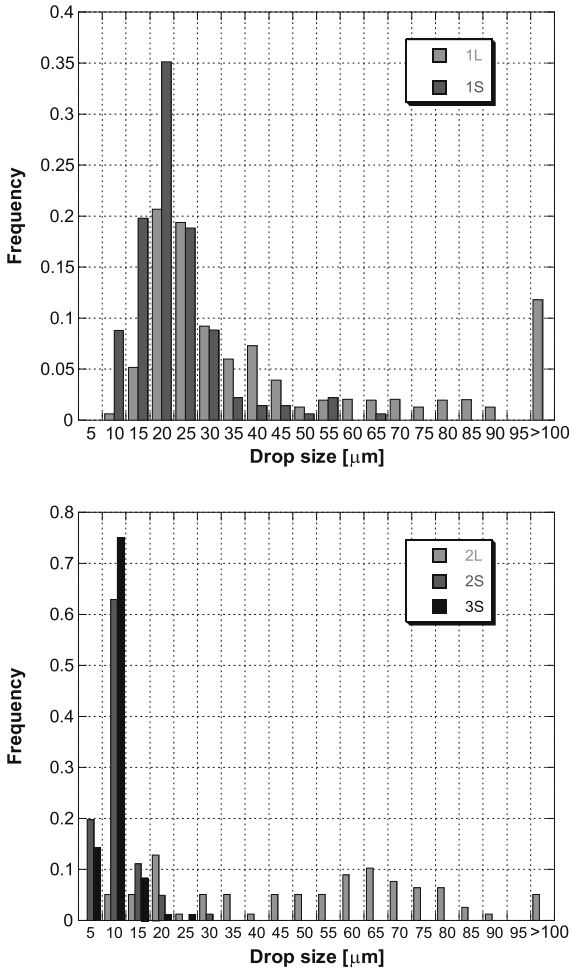

Fig. 1. Drop size distribution for the five emulsions tested.

Table 2
Mean average oil drop radius and standard deviation for all the emulsion systems used in the experiments.

Emulsion	Mean drop diameter (μm)	Standard deviation (μm)
1S	22.2	9.4
1L	42.3	27.6
2S	10.3	4.2
2L	51.5	25.3
3S	9.3	2.7

The shear viscosity of all the fluids as a function of the shear rate was measured using a rotational rheometer, ARES (TA Instruments) with a grooved Couette geometry. The serrated cylinder was used to dissipate slipping effects at the walls, common in the characterization of emulsions and some polymeric solutions, as described by Macosko (1994). The viscosity curve of the continuous phase and of emulsions 1L and 1S are shown in Fig. 2. The polymeric aqueous solution with surfactant behaves as a shear thinning fluid. Both emulsions also exhibit a shear thinning behavior. The emulsion with smaller average drop size and narrower distribution exhibits larger viscosity values than the emulsion with larger drop size and wider drop-size distribution, but the same phase concentration. The larger interfacial area and mutual interaction between different drops increases the viscosity of the emulsion, as explained by Becher (2001). The viscosity curves of emulsions 2L, 2S and 3S are shown in Fig. 3. Once again, the emulsion with smaller drop size is more viscous. As the results for emulsion 3S show, viscosity rises as the concentration of the dispersed phase increases, as expected.

For all the emulsions tested, the viscosity dependence on shear rate at shear rates larger than 1 s^{-1} is well described by a power-law model, namely $\eta = m\dot{\gamma}^{n-1}$. The parameters of the model for the five emulsions are shown in Table 3.

2.2. Experimental procedure

The experimental apparatus used for flow visualization in this work is shown in Fig. 4. A syringe pump is used to feed the emulsion through a quartz capillary at a constant volumetric flow rate. The tubing connecting the syringe to the capillary was made as short and as rigid as possible to minimize the expansion of the tubing as the inlet pressure rises during the experiments. A port, con-

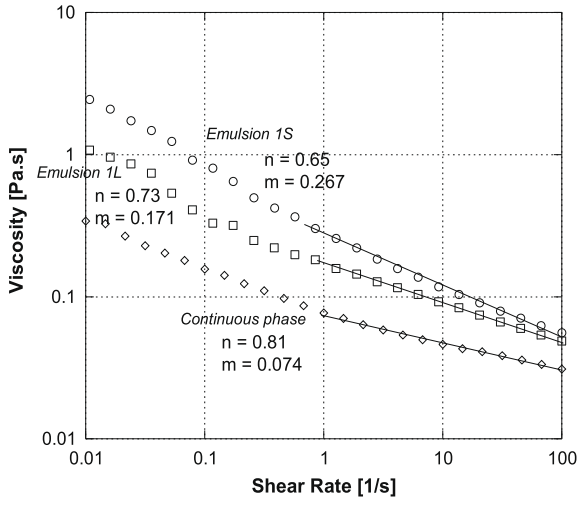

Fig. 2. Shear viscosity as a function of shear rate of the dispersed phase (carbopol solution in water) and emulsions 1S and 1L. *m* and *n* are the power-law model coefficients.

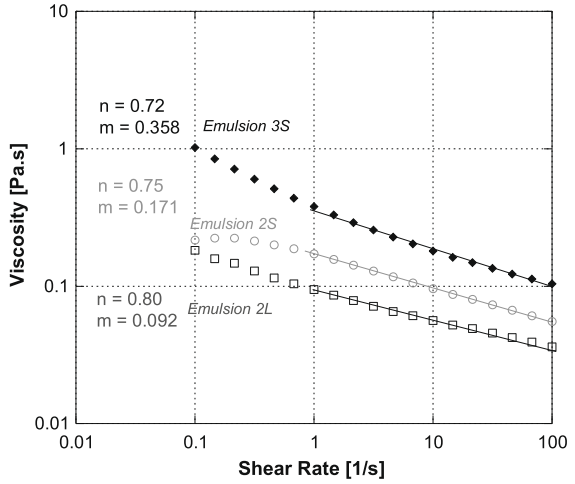

Fig. 3. Shear viscosity as a function of shear rate of emulsions 2S, 2L and 3S. m and n are the power-law model coefficients.

Table 3
Powerlaw model parameters for all emulsions tested.

Emulsion	m (Pa s^n)	n
Continuous phase	0.074	0.81
1S	0.267	0.65
1L	0.171	0.73
2S	0.171	0.75
2L	0.092	0.80
3S	0.358	0.72

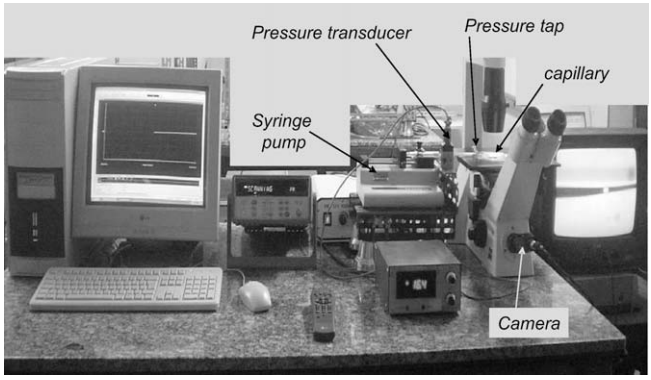

Fig. 4. Photograph of the experimental setup.

nected to a pressure transducer (Validyne), was installed just upstream the capillary tube to measure the pressure drop along the capillary. Pressure values were acquired on the PC by using a multiplexer slot as interface between the transducer and the computer. Pressure data points were taken every second. Systematic error for pressure drop acquisition was ±2%.

The capillary tube was mounted for observation on the platform of an inverted Zeiss Axioplan microscope with a 5× objective. Images were captured in real time and recorded by a CCD camera attached to the microscope and connected directly to the frame grabber, and then recorded on a video tape. The diameters of the glass capillary tube and the neck were equal to 200 and 50 μm, respectively. The length of the capillary was 8 cm and that of the contraction and expansion section was equal to 4 cm. Fig. 5 shows a photograph of the throat section of the capillary tube.

For each emulsion, the flow rate was increased in small steps. At each value of the flow rate, the inlet pressure was measured and

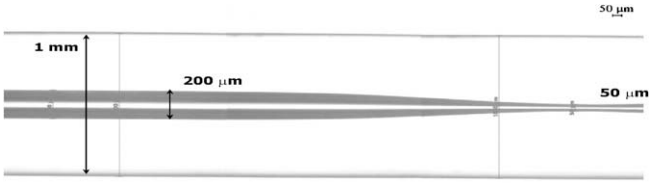

Fig. 5. Photograph of the constricted capillary used as a model of a pore body–pore throat geometry.

the images of the emulsion flowing through the constricted capillary tube were recorded. The range of flow rates explored was chosen such that the average velocity of the liquid flowing through the capillary was similar to the average velocity encountered inside the porous space of oil reservoirs.

3. Results and discussion

For emulsions 1L and 1S, the flow rate explored ranged from $Q = 0.04$ ml/h to $Q = 0.1$ ml/h. The inlet pressure during the experiment for both emulsions is presented in Fig. 6. The flow rate was kept at $Q = 0.04$ ml/h for $t \leqslant 58$ min. At $t = 58$ min, the flow rate was raised to $Q = 0.07$ ml/h, and at $t = 110$ min, it was raised once again to $Q = 0.1$ ml/h. For emulsion 1S, at each flow rate, the pressure stayed almost constant, with only small fluctuations around the average value. After each flow rate change, a new steady state was reached after approximately 9 min. This long transient can be explained by the presence of the compliant tubing that connects the syringe pump to the capillary, by the small dimensions of the capillary and extremely low flow rates explored. Similar behavior has been observed in flows of glycerin–water solutions through micro-capillaries (see Rodd et al., 2005). For the emulsion with large drops 1L, at each flow rate, the pressure difference was higher. At $Q = 0.04$ ml/h, the pressure difference necessary to drive emulsion 1S through the capillary was $\Delta P \approx 2000$ Pa, and to drive emulsion 1L was $\Delta P \approx 4000$ Pa, even though emulsion 1S is more viscous than emulsion 1L. As expected, from these results, it is clear that a continuous model based solely on the emulsion viscosity cannot be used to describe the flow when there are drops larger than the constriction diameter. The presence of oil drops larger than the capillary throat partially obstructs the liquid flow. Another important difference on the behavior of the flow with emulsions 1S and 1L is that the inlet pressure

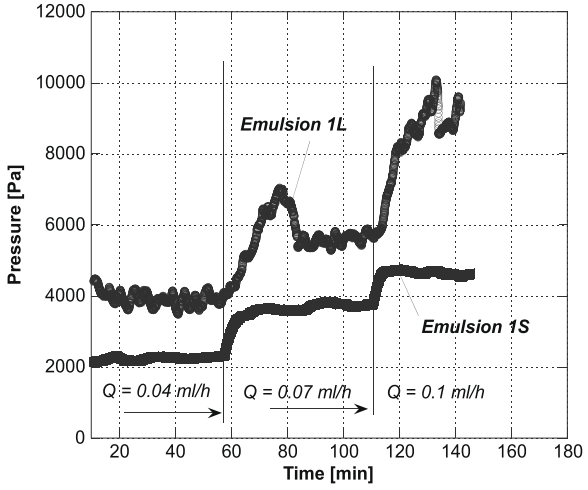

Fig. 6. Evolution of the inlet pressure as the flow rate varies for emulsions 1S and 1L. Range of flow rate: $Q = 0.04$–0.1 ml/h.

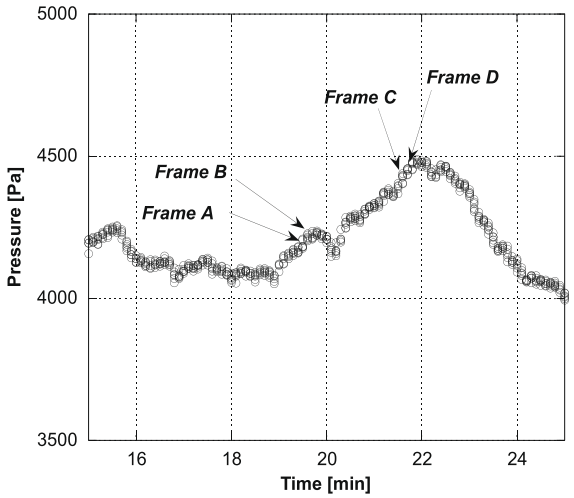

Fig. 7. Evolution of the inlet pressure at $Q = 0.04$ ml/h for emulsion 1L. Images of the flow near the capillary throat at the instants highlighted in this plot are shown in the next figure.

oscillates substantially at a fixed flow rate in the flow of the emulsion with drops larger than the constriction, as was also observed by Olbricht and Leal (1983). They associated the pressure fluctuations with the passage of a single large drop through the capillary throat. Fig. 7 shows the oscillation of the inlet pressure for emulsion 1L at a flow rate $Q = 0.04$ ml/h, between $t = 15$ and 25 min. The images of the flow near the capillary throat at the instants highlighted in Fig. 7 are presented in Fig. 8. A small pressure peak is observed as a drop somewhat larger than the throat diameter passes through the constriction, as observed in frames (a) and (b) of the figure. The deformation of the drop at the constriction is clear in frame (b). A larger pressure peak is observed when a very large drop, much larger than the capillary throat, flows through the constriction, as shown in frames (c) and (d). As the tip of the drop passes through the smallest diameter section, pressure reaches a local maximum value and then drops as the front of the drop moves into the diverging portion of the constriction. A new pressure rise occurs whenever a large drop starts to protrude the capillary throat. This behavior was observed for all emulsions tested here.

The higher average pressure at a fixed flow rate observed when emulsion 1L was used is caused by different mechanisms. As the oil drop flows through the constriction, the radius of curvature of the front of the drop falls, and consequently a higher pressure difference is necessary to overcome the capillary pressure across the drop front interface at the capillary throat, that can be approximated by $\Delta P_{cap} \approx 2\sigma/R_c = 400$ Pa, in this experiment. It is clear that this effect alone does not explain the increased pressure difference necessary to drive the flow. Another mechanism responsible for the pressure rise is the higher interaction between the drop and the capillary wall that occurs with emulsions containing large drops. A third important mechanism is the simple replacement of a less viscous liquid by a more viscous liquid.

The pressure at different flow rates for emulsions 2S and 2L is shown in Fig. 9. The flow range explored went from $Q = 0.04$ to $Q = 0.22$ ml/h. As in the previous example, the flow rate was raised in steps as the inlet pressure was recorded. For the emulsion with small drops 2S, the inlet pressure at each fixed flow rate was virtually constant. For the large drop emulsion 2L, pressure oscillates even when the flow rate is held constant, as also observed in the case of emulsion 1L. However, the amplitude of the oscillation is much larger than that observed with emulsion 1L. This can be explained by the broader drop size distribution and by the higher viscosity of the dispersed phase of emulsion 2L, when compared with emulsion 1L. The pressure oscillation caused by the flow of large oil drops through the capillary throat lasted as long as 10 min in some cases. This rather long time may be explained by the fact that the oil drop flows at a speed slower than the speed of the bulk at the center line. The slower moving large oil drop leads to a local higher concentration of the dispersed phase upstream of the constriction, similar to a filtration process, contributing also to the pressure rise. The fact that a more viscous drop moves slower than the bulk maximum velocity through a capillary has been experimentally observed by Ho and Leal (1975) and predicted by Martinez and Udell (1990). Another possible explanation is that the dispersed phase drops may have coalesced in the syringe before being fed into the capillary. However, we did measure the drop size distribution after the experiments and did not find any evidence of coalescence.

The higher pressure observed with the emulsion with large drops and the amplitude of the pressure oscillation at a fixed flow rate decays as the flow rate rises. At the two highest flow rates explored, $Q = 0.19$ and $Q = 0.22$ ml/h, the average pressure with emulsions 2L and 2S are virtually the same. As the flow rate rises, the capillary number increases and the viscous forces becomes more important relative to surface tension induced forces. Therefore, the extra-pressure required to deform the large drop to squeeze it through the capillary throat becomes negligible, leading to a pressure drop close to that of the emulsion with small drops. Martinez and Udell (1990) predicted that the effect of a single drop flowing through a straight capillary tube on the pressure drop at a fixed flow rate falls with capillary number.

The effect of the dispersed phase concentration on the flow characteristics was evaluated by analyzing the inlet pressure measured in the flow of emulsion 3S, prepared with the same oil and

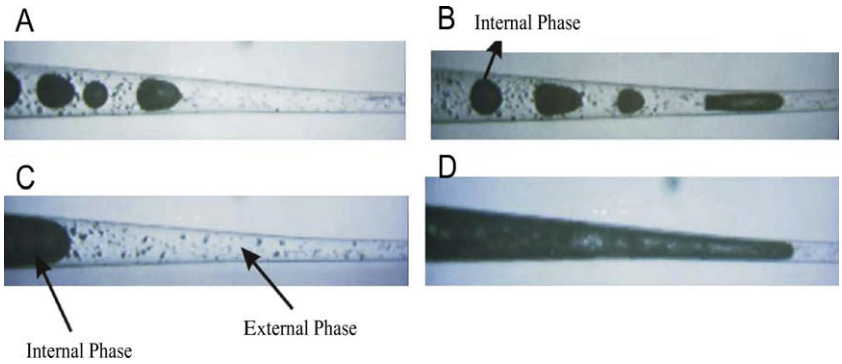

Fig. 8. Images of the emulsion flow just upstream of the capillary throat at the instants highlighted in the previous plot.

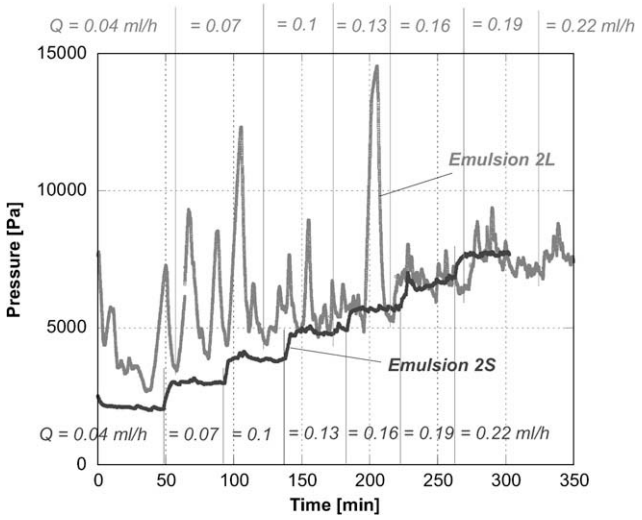

Fig. 9. Evolution of the inlet pressure as the flow rate varies for emulsions 2S and 2L. Range of flow rate: $Q = 0.04$–0.22 ml/h.

procedure of emulsion 2S, but with a oil concentration of 60%. The results are shown in Fig. 10. As in the previous flows with emulsions containing only small drops, pressure is virtually constant at each flow rate, indicating that there is no partial blocking of the capillary throat by the oil drops.

As done by previous authors studying the flow of a single drop immersed in a liquid through a capillary, the flow rate–pressure difference relationship for the emulsion flow through a constricted capillary is analyzed in terms of the extra pressure difference ΔP^+, defined as the measured pressure drop for the emulsion flow less the theoretical Poiseuille pressure drop necessary to drive the continuous phase at the same flow rate. ΔP^+ represents the pressure drop due to the presence of the dispersed phase.

Because the continuous phase is shear thinning and the capillary tube does not have a constant diameter, it is not simple to calculate the Poiseuille pressure difference associated with the flow of the suspending liquid and to define a characteristic value of the continuous phase viscosity, used in the definition of the capillary number.

The pressure drop Δp_c of the continuous phase (a power-law liquid) in the flow through a capillary tube with a diameter that varies along the flow direction can be written in terms of the rheological parameters m and n, the flow rate Q and an equivalent radius $\overline{R}$ that represents an average of the capillary radius

$$\Delta p_c = \left[\frac{Q\left(\frac{1}{n}+3\right)}{\pi \overline{R}^3}\right]^n \frac{2mL}{\overline{R}}. \tag{1}$$

The most appropriate equivalent radius $\overline{R}$ of the capillary for a power-law liquid is defined as

$$\overline{R} \equiv \left\{\frac{L}{\int_0^L \frac{dx}{R(x)^{3n+1}}}\right\}^{\frac{1}{3n+1}}. \tag{2}$$

The image showing the geometry of the capillary, presented in Fig. 5, was digitized and used to evaluate the above integral, using the rheological parameters of the continuous phase, e.g. $m = 0.074$ and $n = 0.81$. The calculated equivalent radius was $\overline{R} = 84.90$ μm.

The characteristic viscosity of the continuous phase μ_c at each flow condition was estimated by the ratio of the wall shear stress τ_w and the wall shear rate $\dot{\gamma}_w$, which for a power-law liquid are given by:

$$\dot{\tau}_w = \frac{\overline{R}\Delta p_c}{2L}, \tag{3}$$

$$\dot{\gamma}_w = \frac{\frac{1}{n}+3}{4n}\frac{4Q}{\pi \overline{R}^3}. \tag{4}$$

The extra-pressure difference ΔP^+, in units of $\mu_c \overline{V}/\overline{R}$, as a function of the capillary number $Ca \equiv \mu_c \overline{V}/\sigma$ for all the emulsions tested are presented in Fig. 11. The error bars indicate the standard deviation of the pressure measurements at each flow rate. A large error bar indicates a large amplitude oscillation of the pressure signal.

The extra pressure ΔP^+ obtained with emulsions with small drops, e.g. emulsions 1S, 2S and 3S, is not a function of the capillary number and does not oscillate. This is the same behavior presented by Olbricht and Leal (1982) and Martinez and Udell (1990) for flow of a single drop through a straight capillary and by Olbricht and Leal (1983) for flow of a single drop through a constricted capillary.

The extra-pressure difference obtained with emulsion 2S, that had the smallest average diameter, approximately 1/5 of the capillary throat, and low concentration (30% by volume) was approxi-

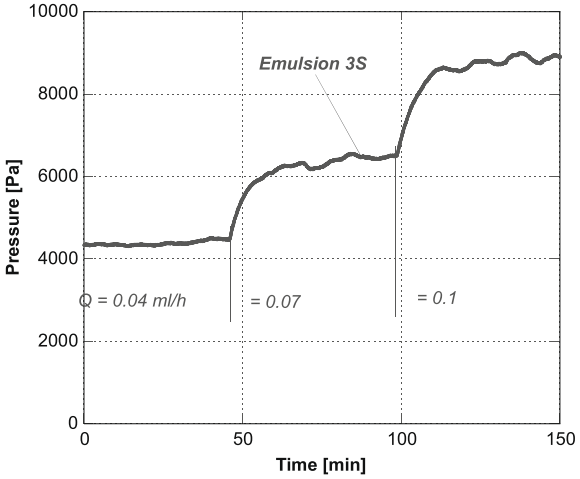

Fig. 10. Evolution of the inlet pressure as the flow rate varies for emulsion 3S. Range of flow rate: $Q = 0.04$–0.1 ml/h.

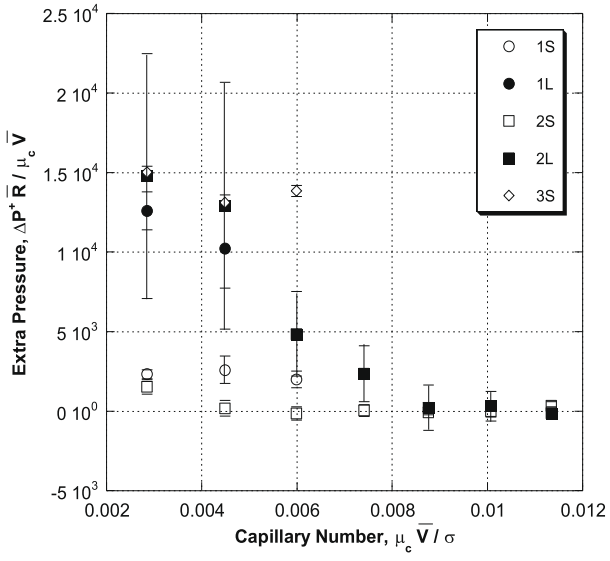

Fig. 11. Extra-pressure difference as a function of the capillary number for the five emulsions tested. The error bars indicate the standard deviation of the measured pressure drop through the capillary.

mately zero, i.e. the presence of the dispersed phase did not alter significantly the flow, when compared to the flow of the continuous phase alone. It is important to observe that the shear viscosity of emulsion 2S, measured in a cone-and-plate fixture in a rotational rheometer, was larger than the continuous phase viscosity, as shown in Fig. 3. As expected, in this length scale, the flow of emulsions cannot be described simply by its viscosity. The extra-pressure rises with the average drop diameter (emulsion 1S) and concentration of the dispersed phase (emulsion 3S).

Because of the smaller capillary diameter used here, closer to that of a high permeability porous media, and the fact that we are not analyzing the flow of a single drop, but of an emulsion, the values of the extra pressure difference measured in this analysis are orders of magnitude higher than those reported before in the literature for the flow of a single drop suspended in the liquid.

The extra pressure difference ΔP^+ obtained with emulsions that have drops larger than the capillary throat diameter (emulsions 1L and 2L) are a strong function of the capillary number. The extra pressure difference falls as the capillary number rises. This behavior was also reported by Olbricht and Leal (1982, 1983). Again the values of the extra pressure difference measured here are orders of magnitude larger because of the much smaller capillary diameter, capillary number and viscosity of the dispersed phase used in this work.

The comparison between the measured extra-pressure difference with emulsions 2S and 2L reveals an interesting phenomena, not reported before. At low capillary number, e.g. $Ca < 0.008$, ΔP^+ with emulsion 2L is much larger than that obtained with emulsion 2S. At capillary numbers above this critical value, the pressure gradient–flow rate relationship for both emulsions is virtually the same. As discussed before, at high capillary number, the surface tension induced force is negligible and so is the extra pressure needed to deform the drop. The partial pore blocking mechanism, that represents the larger extra-pressure difference, related to the presence of large drops on the injected emulsion, that may explain the improved reservoir sweep observed in some experiments, only occurs if the local capillary number is below a critical value that is a function of the emulsion properties. In this case, it is $Ca_c \approx 0.008$. If the emulsion properties and process conditions are such that the local capillary number is higher than this value, there is no pore blocking on an oil recovery operation. This dependence on capillary number may be used in order to define the location where the partial pore blocking should occur in the reservoir. This can be accomplished by tuning the emulsion properties, such as interfacial tension, viscosity ratio and drop size distribution, in order to have the critical capillary number below which the mobility reduction occurs coinciding with the local capillary number at the displacement front.

These results can be used in the development of a capillary network model for the flow of emulsions in porous media. The flow in each capillary q can be described in terms of the mobility of the capillary and the pressure difference applied to its extremities Δp:

$$q = fK_c \frac{\Delta p}{L}, \tag{5}$$

where K_c is the mobility of the flow of the continuous phase alone and f is a scaling factor to account for the partial pore blocking, defined as the ratio of the Poiseuille pressure difference necessary to drive the flow of the continuous phase alone to the one associated with the emulsion flow at the same flow rate:

$$f = \frac{\Delta p_c}{\Delta p}. \tag{6}$$

Fig. 12 shows the scaling factor as a function of the capillary number for the five emulsions tested in the experiments. These results are equivalent to those presented in Fig. 11, but now the change in the flow due to the presence of the dispersed phase is presented in terms of the ratio between the pressure differences, not the difference between them. Further investigation is necessary in order to construct a complete description on how the scaling factor f varies with the emulsion concentration, viscosity ratio, drop size distribution and capillary number.

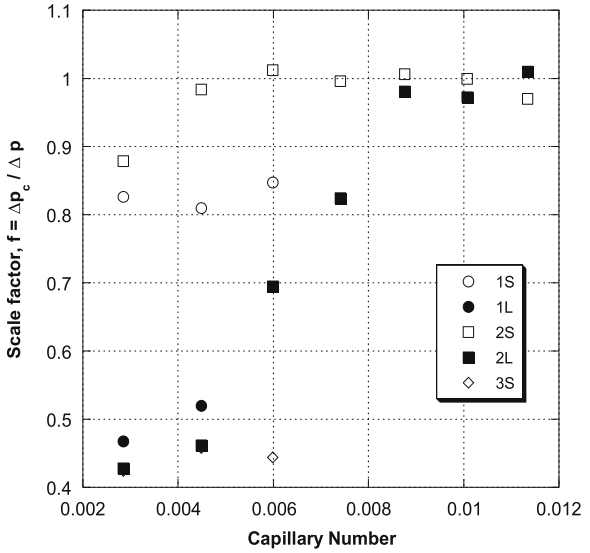

Fig. 12. Scale factor to be used on the definition of the capillary mobility for flow of emulsions.

4. Summary

The flow of oil-in-water emulsions through a pore-throat model, represented by a converging–diverging quartz capillary tube, has been characterized by the pressure–drop flow rate response. The flow response characterization has been paired with simultaneous visualization under an optical microscope. The effect of the diameter of the dispersed phase on the pressure drop was analyzed by comparing the response of two emulsions with the same volumetric dispersed phase fraction, but with different drop size distribution; one with an average drop diameter smaller and the other larger than the narrowest section of the capillary. The results indicate that even for the relatively smooth geometry of the constricted capillary employed, the flow of emulsion is dominated by blocking mechanisms caused by drops larger than the capillary.

Blockage of the pore-throat or constriction in the quartz model signals abrupt pressure oscillations, which are directly associated with the passage of large drops through the capillary throat. The increased curvature of the drop tip as it approaches the narrowest section of the capillary tube leads to pressure peaks, followed by pressure relaxation. However, as the capillary number is increased, leading to larger viscous effects, the average pressure response for the coarser emulsion approaches that of the smaller-radius emulsions.

The blocking mechanism has been characterized by comparing the average measured response to that of flow of the continuous phase alone. The results indicate the effect of the dispersed phase in the flow and that, as expected, the flow of emulsions through micro-capillaries cannot be described by its viscosity alone. A two-phase flow analysis is needed.

We speculate that as emulsions used for enhanced-oil recovery operations flow through reservoir rocks, they act as dynamic mobility control agents, by blocking water paths and diverting the displacing fluid toward upswept regions of the porous medium.

This mechanism requires further investigation, but the results presented here will serve to build network models to develop further understanding of flow of emulsions through porous media.

Acknowledgements

S.C. would like to thank ANP for support through his doctor's degree scholarship. This research was funded by grants from the Brazilian Research Council (CNPq) and Petrobras.

References

Abou-Kassem, J.H., Farouq Ali, S.M., 1995. J. Can. Petrol. Technol. 34, 30–38.
Alvarado, D.A., Marsden, S.S., 1979. SPE J. 19, 369–377.
Bai, B., Han, M., Li, Y., Wei, M., Gao, Y., Cost, J.-P., 2000. In: SPE/DOE 59320, Proceedings of the 24th SPE/DOE Symposium on IOR, Tulsa, OK, USA, pp. 1–7.
Becher, P., 2001. Emulsions: Theory and Practice. Oxford University Press, Oxford.
Ho, B.P., Leal, G., 1975. J. Fluid Mech. 71, 361–384.
Hofman, J.A.M.H., Stein, H.N., 1991. Colloids Surf. 61, 317–329.
Islam, M.R., Farouq Ali, S.M., 1994. J. Can. Petrol. Technol. 33, 59–63.
Jain, V., Demond, A.H., 2002. Environ. Sci. Technol. 36, 5426–5433.
Khambhratana, F., Thomas, S., Farouq Ali, S.M., 1997. In: SPE 39033, Proceedings of the Fifth Latin American and Caribbean Petroleum Engineering Conf. and Exhibition, Rio de Janeiro, Brazil, pp. 1–16.
Khambhratana, F., Thomas, S., and Farouq Ali, S.M. 1998. In: SPE 48910, Proceedings of the 1998 SPE Conference and Exhibition in China, Beijing, China, pp. 657–665.
Kokal, S., 2005. SPE Prod. Facil. 20, 5–13.
Macosko, C.W., 1994. Rheology: Principles, Measurements, and Applications. Wiley–VCH, New York.
Martinez, M.J., Udell, K.S., 1990. J. Fluid Mech. 210, 565–591.
McAuliffe, C.D., 1973a. J. Petrol. Technol. 25, 721–726.
McAuliffe, C.D., 1973b. J. Petrol. Technol. 25, 727–733.
Olbricht, W.L., Leal, G., 1982. J. Fluid Mech. 115, 187–216.
Olbricht, W.L., Leal, G., 1983. J. Fluid Mech. 134, 329–355.
Rodd, L.E., Scott, T.P., Boger, D.V., Cooper-White, J.J., McKinley, G.H., 2005. J. Non-Newton. Fluid Mech. 129, 1–22.
Romero, L., Zirit, J.L., Marín, A., Rojas, F., Mogollón, J.L., Manrique, E., Paz, F., 1996. In: SPE/DOE 35461, Proceedings of the Tenth Symposium on IOR, Tulsa, OK, USA, pp. 611–621.
Sarma, H.K., Maini, B.B., Jha, K., 1998. J. Can. Petrol. Technol. 37, 55–62.
Seright, R.S., Liang, J., 1995. In: SPE 30120, Proceedings of the European Formation Damage Conference, The Hague, The Netherlands, pp. 431–440.
Soo, H., Radke, C.J., 1984. Ind. Eng. Chem. Fund. 23, 342–347.
Soo, H., Radke, C.J., 1986. Chem. Eng. Sci. 41, 263–272.
Soo, H., Williams, M.C., Radke, C.J., 1986. Chem. Eng. Sci. 41, 273–281.
Tsai, T.M., Miksis, M.J., 1994. J. Fluid Mech. 274, 197–217.